Solutions to an association field model on the retinal sphere: sub-Riemannian geodesics in SO(3) with cuspless spherical projections

Alexey Mashtakov (alexey.mashtakov@gmail.com), Remco Duits (R.Duits@tue.nl),
Yuri Sachkov (sachkov@sys.botik.ru), Ivan Beschastnyi(i.beschastnyi@gmail.com)

Eindhoven University of Technology, The Netherlands; Program Systems Institute of RAS, Pereslavl-Zalessky, Russia

Summary

We consider the problem $\mathbf{P_{curve}(S^2)}$ of minimizing $\int_0^l \sqrt{\xi^2 + k_g^2(s)}\, ds$ for a curve $[0, l] \ni s \mapsto \mathbf{n}(s) \in \mathbf{S^2}$, with free length l and geodesic curvature k_g, on $\mathbf{S^2}$ with fixed boundary points and directions. This problem is a natural spherical extension of a flat model of primary visual cortex. We are motivated by the fact that the retina is not flat, which is important both for cortical modeling and for processing retinal images. We derive stationary curves for general case $\xi > 0$.
Stationary curves in considered problem can be used for retinal vessel tracking on a spherical image of a retina. We compute stationary curves as projections of sub-Riemannian geodesics in left-invariant problem on $\mathbf{SO(3)}$. In such a way, this work continues to study application of Sub-Riemannian geodesics to image analysis.
We analyze cusp points and evaluate the first cusp time, i.e. the instance of time where the spherical projection of a sub-Riemannian geodesic has a cusp.

Statement of $P_{curve}(S^2)$ problem

Given $\quad S^2 = \{\mathbf{n} \in \mathbb{R}^3 \,|\, \|\mathbf{n}\| = 1\}$

$\xi > 0$ $\mathbf{n}_i \in \mathbf{S^2}$, $i \in \{0, 1\}$,
$\mathbf{n}'_i \in T_{\mathbf{n}_i}\mathbf{S^2}$, $\quad \|\mathbf{n}'_i\| = 1$.

To Find $\mathbf{n} : [0, l] \to \mathbf{S^2}$ s.t.

$$\mathbf{n}(0) = \mathbf{n}_0, \quad \mathbf{n}(l) = \mathbf{n}_1,$$
$$\mathbf{n}'(0) = \mathbf{n}'_0, \quad \mathbf{n}'(l) = \mathbf{n}'_1,$$
$$\int_0^l \sqrt{\xi^2 + k_g^2(s)}\, ds \to \min$$

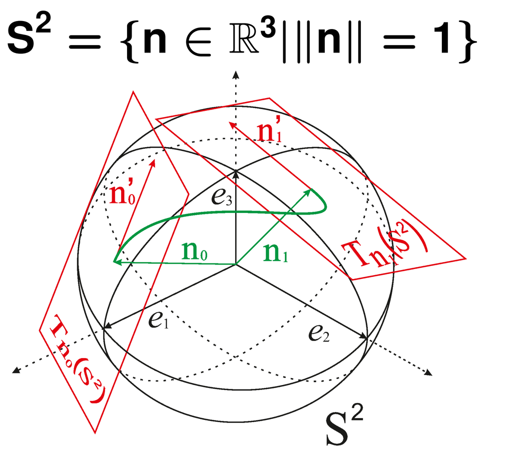

$$s = \int_0^s 1 ds' = \int_0^s \|\mathbf{n}'(s')\| ds',$$
$$k_g(s) = \mathbf{n}''(s) \cdot (\mathbf{n}(s) \times \mathbf{n}'(s)).$$

Statement of P_{mec} problem

Left-invariant sub-Riemannian problem on $\mathbf{SO(3)}$

$$\dot{R} = -u_1 R A_2 + u_2 R A_1, R(0) = \mathrm{Id}, R(t_1) = R_1, R \in \mathrm{SO(3)},$$
$$\mathfrak{E}(R(\cdot)) = \int_0^{t_1} \sqrt{\xi^2 u_1^2 + u_2^2}\, dt \to \min, \; (u_1, u_2) \in \mathbb{R}^2, \xi > 0.$$

We parameterize $\mathbf{SO(3)} \ni R(x, y, \theta) = e^{yA_3} e^{-xA_2} e^{\theta A_1}$, where $(x, y, \theta) \in [-\pi/2, \pi/2] \times \mathbb{R}/\{2\pi\mathbb{Z}\} \times \mathbb{R}/\{2\pi\mathbb{Z}\}$, and use the map projection from $\mathbf{SO(3)} \ni R \mapsto Re_1 \in \mathbf{S^2}$.

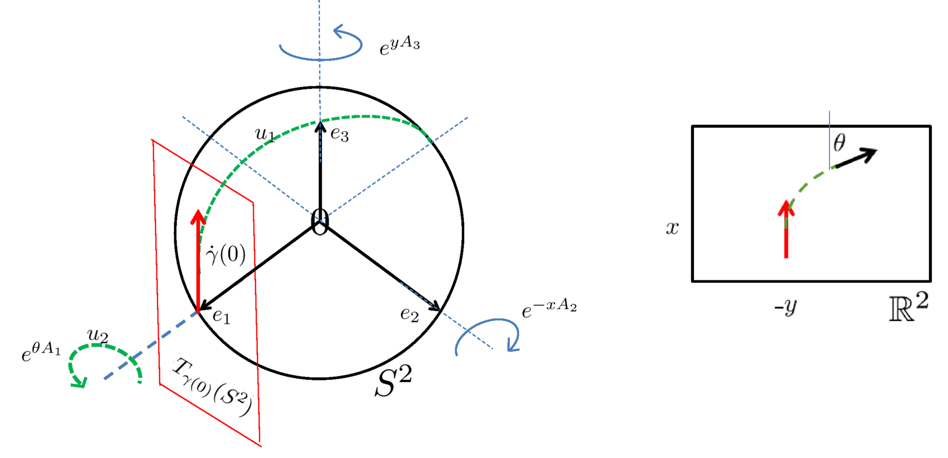

Connection P_{mec} and $P_{curve}(S^2)$

Let $R_{\min}$ be a smooth minimizer of $\mathbf{P_{mec}}$ without cusp. Set

$$\begin{cases} R_{\min}(t_1)e_1 = \mathbf{n}_1 = R_{fin}e_1, \\ R_{\min}(t_1)e_3 = \mathbf{n}'_1 = R_{fin}e_3, \\ \mathbf{n}_0 = e_1, \quad \mathbf{n}'_0 = e_3. \end{cases}$$

Then for such boundary conditions $\mathbf{P_{curve}}$ is well-posed and

$$\mathbf{n}(s) = R_{\min}(t(s))e_1, \quad \begin{cases} u_1 = \frac{ds}{dt}, \\ u_2 = k_g \frac{ds}{dt}, \end{cases}$$

with $t(s) = \int_0^s \sqrt{\xi^2 + k_g^2(\sigma)}\, d\sigma$, for all $0 < s \le l < s_{\max}$, and $t_1 = t(l)$. Here s_{max} is 1-st positive root of $u_1(s) = 0$.

Optimal control problem on $S^2 \times S^1$

Apply PMP to problem $\mathbf{P_{mec}}$:

$$\dot{\nu} = u_1 X_1 + u_2 X_2, \quad \nu(0) = \nu_0, \; \nu(T) = \nu_1, \; (u_1, u_2) \in \mathbb{R}^2,$$
$$\tilde{\mathfrak{E}} = \int_0^T \frac{(\xi^2 u_1^2 + u_2^2)}{2}\, dt \to \min, \quad \nu \in \mathbf{S}^2_{x,y} \times \mathbf{S}^1_\theta, \quad \xi > 0,$$

where $\nu = (x, y, \theta)^T$, $\nu_0 = (0, 0, 0)^T$ and
$X_1 = (\cos\theta, -\sec x \sin\theta, \sin\theta \tan x)^T$, $X_2 = (0, 0, 1)^T$.

The Hamiltonian system of PMP

$$\begin{cases} \dot{h}_1 = -h_2 h_3, \\ \dot{h}_2 = \frac{1}{\xi^2} h_1 h_3, \\ \dot{h}_3 = \left(1 - \frac{1}{\xi^2}\right) h_1 h_2, \end{cases} \qquad \begin{cases} \dot{x} = \frac{h_1}{\xi^2} \cos\theta, \\ \dot{y} = -\frac{h_1}{\xi^2} \sec x \sin\theta, \\ \dot{\theta} = \frac{h_1}{\xi^2} \sin\theta \tan x + h_2. \end{cases}$$

vertical part $\qquad$ horizontal part

Vertical part

In SR-arclength parametrization vertical part is equivalent to equation of the mathematical pendulum $\ddot{\beta} = -r \sin\beta$, that was integrated explicitly in terms of Jacobi elliptic functions. Here $h_1 = \xi \cos\beta/2$, $h_2 = \sin\beta/2$, $h_3 = \frac{1}{2}\xi\dot{\beta}$, $r = \frac{1}{\xi^2} - 1$.
Integral Manifolds: the Hamiltonian (green), $\|h\|^2$ (red), and the full energy of pendulum (blue)

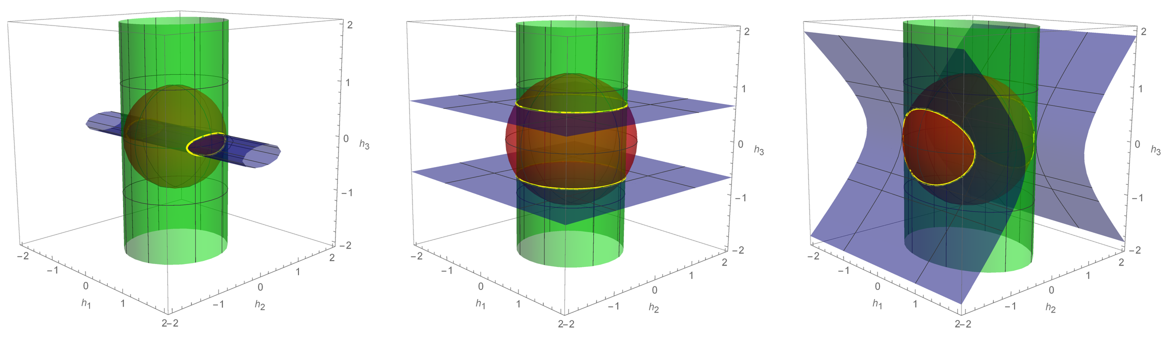

Elliptic $\xi < 1$ $\qquad$ Linear $\xi = 1$ $\qquad$ Hyperbolic $\xi > 1$

In spherical arclength vertical part reduces to linear

$$h'_2(s) = h_3(s), \quad h'_3(s) = (\xi^2 - 1)h_2(s).$$

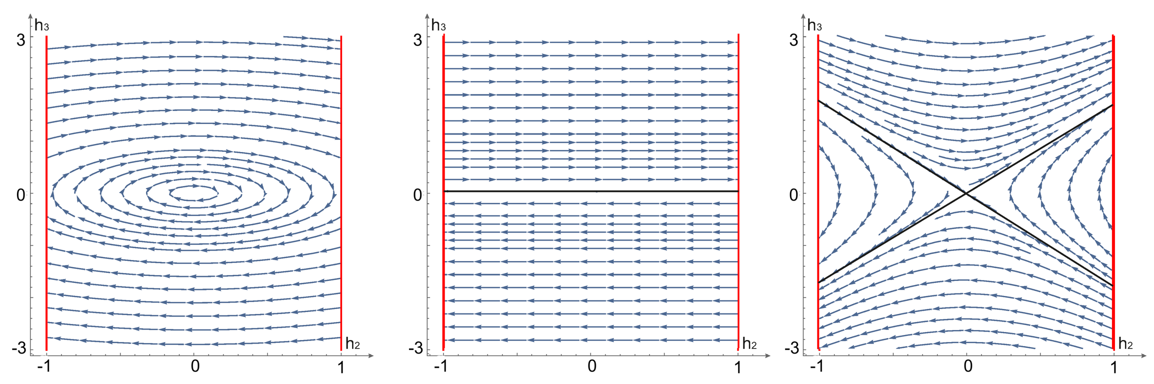

Evaluation of first cusp time

In linear case $s_{\max}(h_{20}, h_{30}) = \frac{\mathrm{sgn}(h_{30}) - h_{20}}{h_{30}}$.
Define $\chi = \sqrt{\xi^2 - 1}$. In elliptic and hyperbolic cases

$$s_{\max}(\chi, h_{20}, h_{30}) = \begin{cases} +\infty \text{ for } \kappa < 0 \text{ or } h_{20}\chi + h_{30} = 0, \\ \frac{1}{\chi} \log\left(\frac{s_1(\sqrt{\kappa} + \chi)}{h_{20}\chi + h_{30}}\right) \text{ otherwise.} \end{cases}$$

$$s_1 = \mathrm{sgn}\,(\mathrm{Re}\,(h_{20}\chi + h_{30})), \; \kappa = h_{30}^2 + (1 - h_{20})^2 \chi^2 \in \mathbb{R}.$$

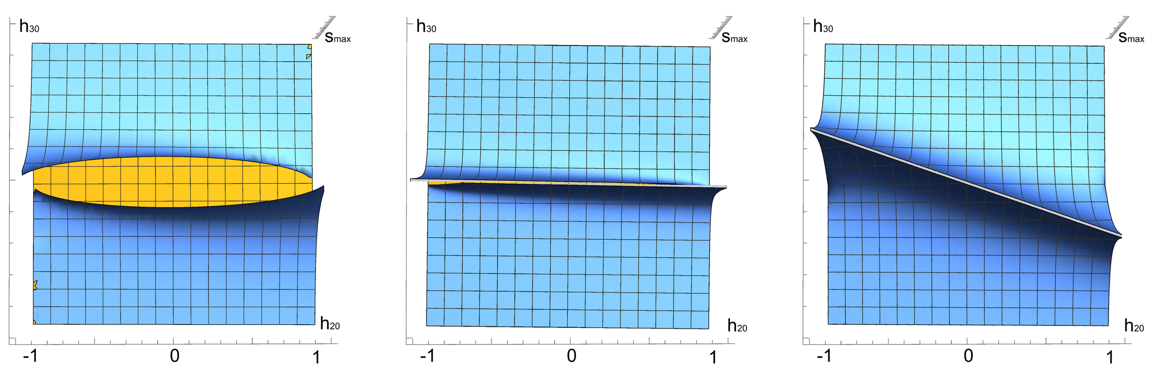

Horizontal part

Horizontal part was explicitly integrated in terms of Jacobi elliptic functions and elliptic integral of the third kind. Similar formula are obtained as in $\mathbf{SE(2)}$ case.

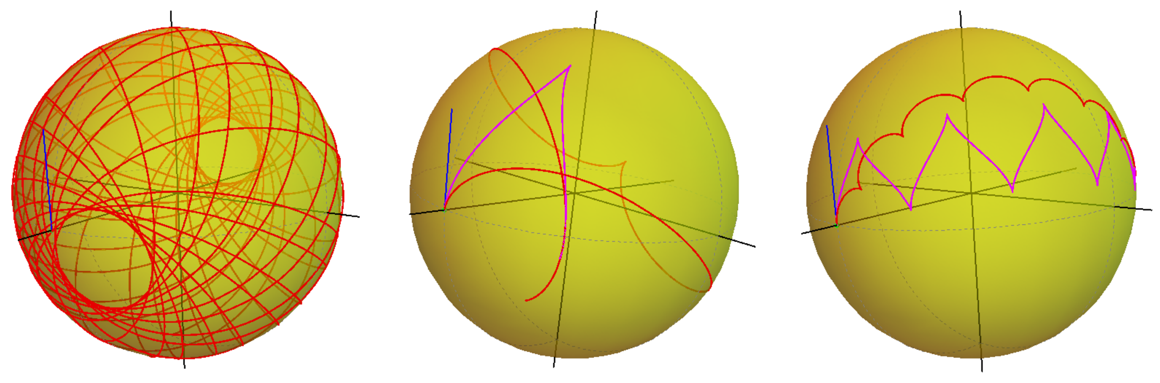

Projections of cuspless extremal trajectories on $\mathbf{S^2}$

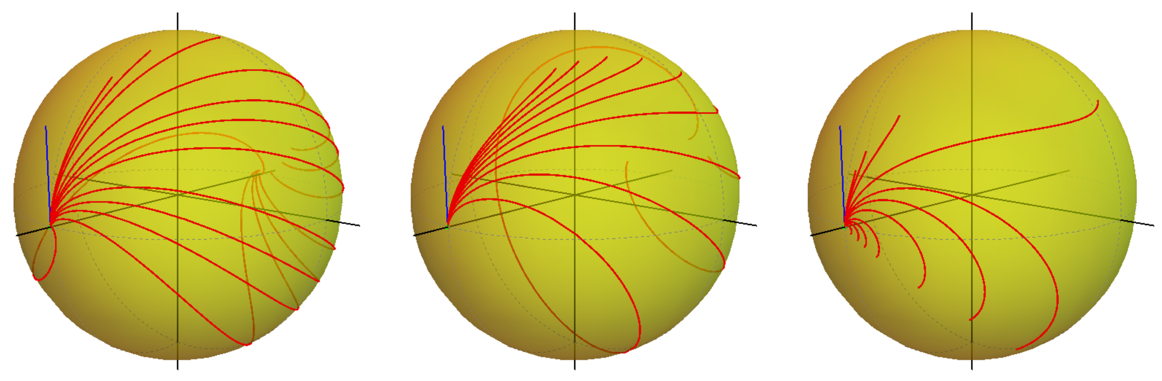

Elliptic $\xi < 1$ $\qquad$ Linear $\xi = 1$ $\qquad$ Hyperbolic $\xi > 1$

Asymptotics of 1st conjugate time

Asymptotics near stable equilibrium of the pendulum

$$t^1_{conj} = \frac{2\pi}{\sqrt{r}} - 2\left((\varphi_0 + \frac{\pi}{2\sqrt{r}}) \mod \frac{\pi}{\sqrt{r}}\right).$$

where $\sqrt{r} = \sqrt{\frac{1}{\xi^2} - 1}$, $s_1 = \mathrm{sgn}\, h_{10}$,

$$\varphi_0 = \frac{1}{\sqrt{r}} F\left(\arg\left(\frac{h_{30}}{\sqrt{\xi^2 - 1}} + i\frac{s_1 h_{20}}{k}\right), k^2\right), \; k = \sqrt{h_{20}^2 + \frac{h_{30}^2}{1 - \xi^2}}$$

Wave front

Wave fronts in $\mathbf{P_{mec}(S^2)}$ in elliptic (green), linear (red) and hyperbolic (blue) cases. Comparison with $\mathbf{SE(2)}$ shows local similarity of wave fronts in $\mathbf{SE(2)}$ and $\mathbf{SO(3)}$.

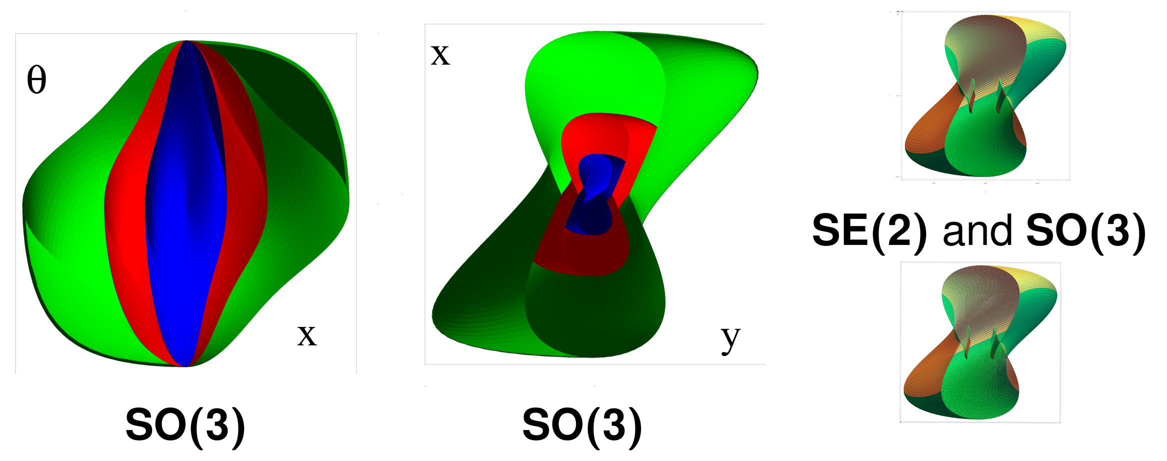

SO(3) $\qquad$ SO(3) $\qquad$ SE(2) and SO(3)

Cusp surfaces in linear case

Red surface: endpoints of geodesics starting from cusp.
Blue surface: endpoints of geodesics ending in cusp.
In $\mathbf{SO(3)}$ case:

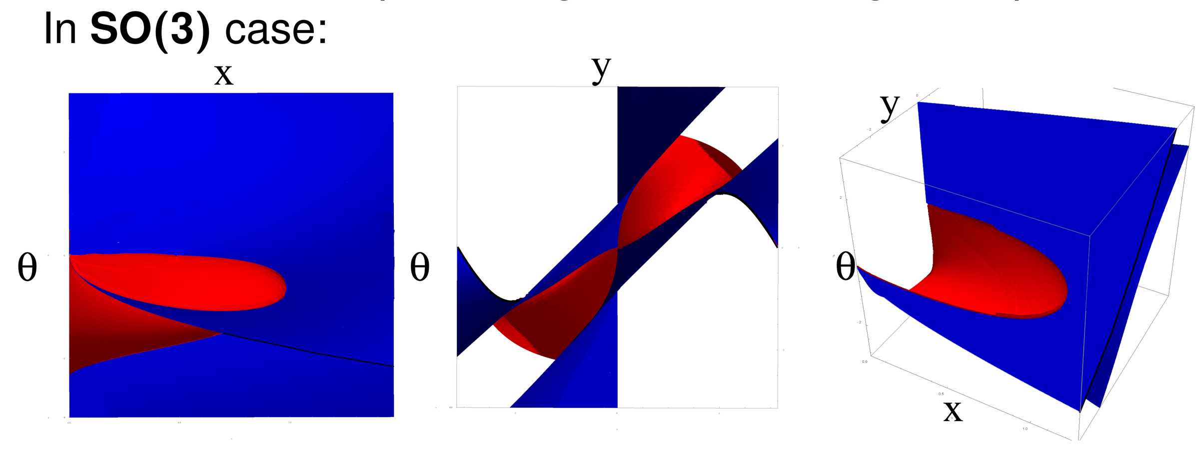

In $\mathbf{SE(2)}$ case:

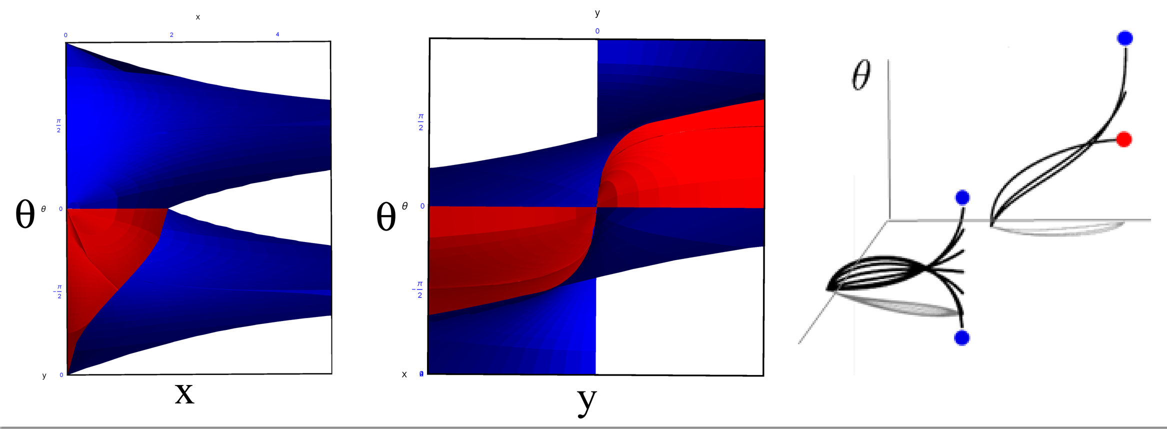

Plans

We plan to generalize our wavefront propagation algorithm to $\mathbf{SO(3)}$, that would solve boundary values problem in $\mathbf{P_{curve}(S^2)}$. Then use it for enhancement of spherical photos including external cost $C(\gamma(s)) = C(\mathbf{n}(s), \mathbf{n}'(s))$ of retina and for retinal vessel tracking.

Bibliography

[1] J.Petitot, The neurogeometry of pinwheels as a sub-Riemannian contact structure, J. Physiology, 2003.

[2] G. Citti, A. Sarti, A cortical based model of perceptual completion in the roto-translation space, JMIV, 2006.

[3] U. Boscain, F. Rossi, Projective Reed-Shepp Car on S^2, ESAIM COCV, 2009.

[4] A.P. Mashtakov, A.A. Ardentov, Y.L. Sachkov, Parallel Algorithm and Software for Image Inpainting via Sub-Riemannian Minimizers on the Group of Rototranslations, NMTMA, 2013.

[5] R. Duits, U. Boscain, F. Rossi, Y. Sachkov, Association fields via cuspless sub-Riemannian geodesics in SE(2), JMIV, 2014.

[6] E. Bekkers, R. Duits, T. Berendschot, B.H. Romeny, A Multi-Orientation Analysis Approach to Retinal Vessel Tracking, JMIV, 2014.

[7] E. Bekkers, R. Duits, A. Mashtakov, G. Sanguinetti, Solving Sub-Riemannian Geodesics in SE(2) with External Cost, Submitted to SSVM 2014.

Conclusion

The topological behavior in phase space is very different for $\xi < 1$, $\xi = 1$ and $\xi > 1$. The curvature of the sphere affects the range $\mathfrak{R} = \{\mathrm{Exp}(\lambda_0, t) | t \le t_{cusp}(\lambda_0)\}$ of the exponential map of $\mathbf{P_{curve}(S^2)}$ considerably in comparison to $\mathbf{P_{curve}(\mathbb{R}^2)}$. It is remarkable, that in contrast to $\mathbf{P_{curve}(\mathbb{R}^2)}$ there exist nonoptimal cuspless sub-Riemannian geodesics (but they typically cross the equator). We obtained expression for SR-geodesics in $\mathbf{P_{mec}(S^2)}$, using parametrization $\mathbf{SO(3)} \ni R(x, y, \theta) = e^{yA_3} e^{-xA_2} e^{\theta A_1}$, motivated by analogy to $\mathbf{SE(2)}$. We evaluated first cusp time and studied the range of exponential map. Based on these results, we plan to develop an algorithm, that solves boundary values problem in $\mathbf{P_{curve}(S^2)}$. Then use it for enhancement of spherical photos of retina including external cost $C(\gamma(s)) = C(\mathbf{n}(s), \mathbf{n}'(s))$ and for retinal vessel tracking.